Towards commonality between shear banding and glass-liquid transition in metallic glasses

Zeng-Yu Yang [1,2] and Lan-Hong Dai [1,2,3,*]

[1]*State Key Laboratory of Nonlinear Mechanics, Institute of Mechanics, Chinese Academy of Sciences, Beijing 100190, China*
[2]*School of Engineering Science, University of Chinese Academy of Sciences, Beijing 100049, China*
[3]*School of Future Technology, University of Chinese Academy of Sciences, Beijing 100049, China*

Despite the high attendance of shear banding in metallic glasses and other disordered materials, the nature of the emergence of shear band is still mysterious. Using molecular dynamics simulations, a set of detailed characterizations of shear band in a typical $Cu_{50}Zr_{50}$ metallic glass is obtained. Then we uncover a large number of robust and intriguing commonalities between the emergence of shear bands and the glass-to-liquid transition, including strong similarities on viscosity drop, enthalpy discontinuity, breakdown of hard backbone network, as well as relaxation process. Such observations indicate that shear banding in metallic glasses is a consequence of deformation-controlled glass transition, as further quantitatively validated via the compelling overlap between the venerable Vogel-Fulcher-Tammann law (and Adam-Gibbs relation) and the evolving glass state of shear band controlled by configurational temperature. These results provide a direct bridge between shear banding and glass-to-liquid transition and are instrumental to build the unified framework of flow behavior induced either by thermal or stressed stimuli in disordered materials.

Shear banding behavior with severe plastic strain localized in extremely thin strip regions is one of the most important causes of catastrophic failure and also a recent topic of intense discussion in disordered materials, ranging from glasses, polymers, colloids, and granular solids [1–6]. The initiation of shear band in metallic glasses is so far considered as a self-feedback process, in which the local activation of flow defect [7,8] or shear transformation zone (STZ) [9,10] with characteristic density variations [11] is followed by the strain aggregation, subsequent percolation of deformed regions, and ultimate shear band formation [12–16]. This physical evolving picture has recently been further fulfilled by decoupling the plastic unit as the more careful concepts as shear-dominated zone, dilatation-dominated zone, and rotation-dominated zone [17]. Despite its notable progress in providing the explanation of shear banding emergence, the current dominant paradigm mainly focuses on the strain field, causing the absence of a thorough understanding of shear banding nature, especially from the perspective of inhomogeneous dynamic evolution [18]. The understanding of the nature of shear banding and the cause of the dynamic burst in the vicinity of the yielding point remain limited. The preceding work of Guan *et al.* [19] provides a novel indication that temperature and stress share the similar effects on controlling the viscosity. This work offers an alternative view for deformation of metallic glasses. However, since it is based on the steady-state flow, the more fundamental understanding of shear banding emergence remains an issue yet to be resolved. In this Letter we disclose the intimate connection between stress induced shear banding flow and thermal glass-to-liquid transition based on atomistic simulations. It is demonstrated that shear banding shows intriguing similarities with glass-to-liquid transition on viscosity drop, enthalpy discontinuity, structural evolution, and relaxation behavior. Such correlation is further quantitatively confirmed via the stringent tests of thermodynamic theories of the glass transition, such as the Vogel-Fulcher-Tammann equation and the Adam-Gibbs relation [20], on the glass state of shear band. These rich evidences figure out the mysterious mask of shear banding, manifesting as the deformation-controlled glass-to-liquid transition, taking place in the exact localized regions.

To investigate the linkage between glass transition and shear banding phenomenon, we carry out a series of molecular dynamics simulations via LAMMPS code [21]. The prototypical binary $Cu_{50}Zr_{50}$, containing 121,500 atoms, is used as the model glass with the embedded-atom potential [22] employed to describe the atomic interactions. On the one hand, the nature of glass transition is characterized by monitoring the quenching process, in which the model glass is prepared. On the other hand, the simple shear test of $Cu_{50}Zr_{50}$ glass is conducted to capture the inhomogeneous deformation and trace the shear banding behavior. Then the deformed glasses at strains right prior to the onset of shear band (far away from the elastic regime) are used for the relaxation process. Further details of the atomistic simulations can be obtained in the Supplemental Material [23] (see also Refs. [24,25] therein).

Figure 1 shows the overall similarity between the shear banding behavior and thermally driven glass transition. First of all, typical stress-strain curve of modeled $Cu_{50}Zr_{50}$ glass under simple shear test is given in Fig. 1(a), in which stress overshoot [26] is markedly visible and points out the occurrence of plastic instability, i.e., shear banding. It should be
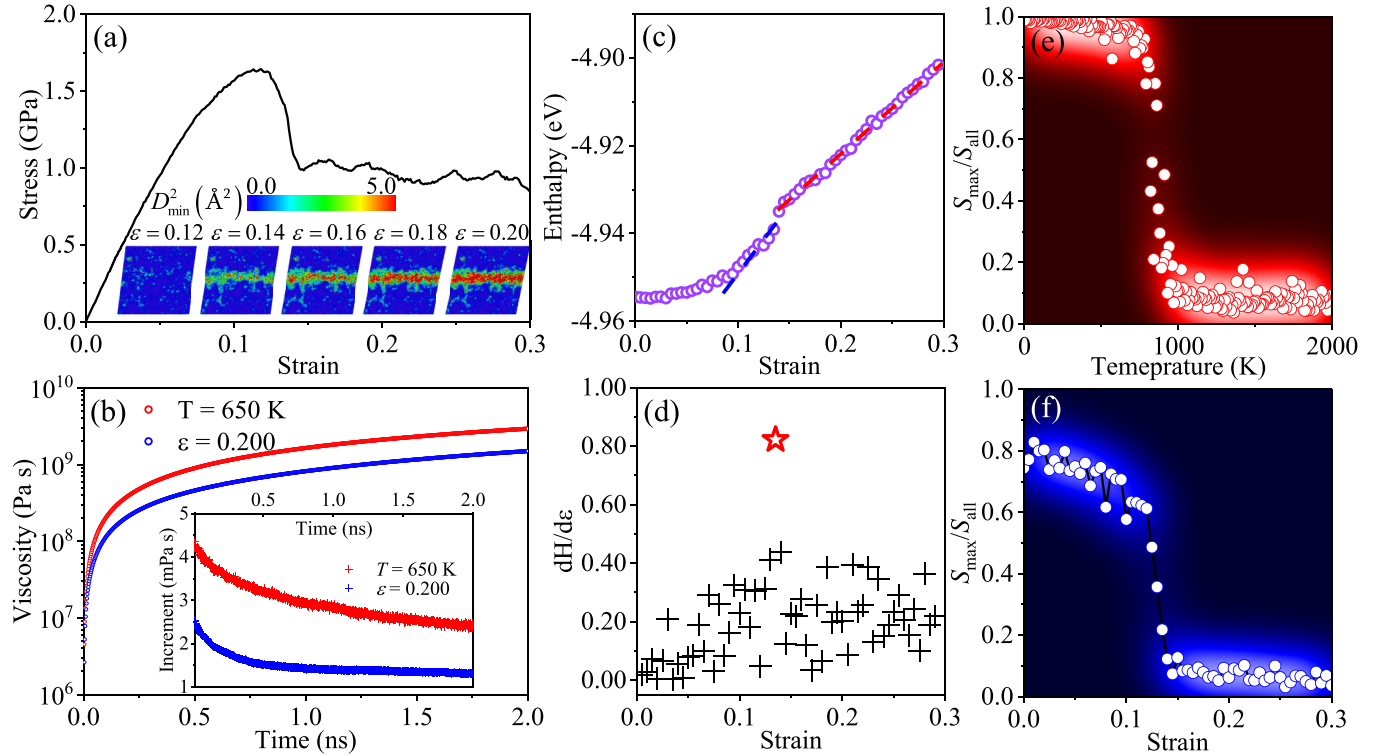
*lhdai@lnm.imech.ac.cn

FIG. 1. Resemblance between shear banding and glass-to-liquid transition in metallic glass. (a) Typical stress-strain curve of $Cu_{50}Zr_{50}$ metallic glass under simple shear loading. The insets are deformation patterns (colored according to D_{min}^2) at various strains ranging from 0.12 to 0.20 with strain interval of 0.02. (b) Calculation of shear viscosity via Green-Kob theorem for mature shear band at strain of 0.2 as well as supercooled liquid at glass transition temperature, i.e., 650 K, respectively. The inset shows the variation of shear auto-correlation function as a function of relaxation time. (c) The enthalpy per atom as a function of applied strain. (d) Slope of enthalpy-strain plot in (c). (e) Temperature dependence of interpenetrating factor S_{max}/S_{all} for modeled $Cu_{50}Zr_{50}$ system during quenching process. (f) S_{max}/S_{all} as a function of applied strain for atoms residing in shear band.

noted that the use of stress overshoot to characterize shear band may be no longer valid in experiments where stress overshoot usually takes place at high temperatures and slow strain rates, and is a measure of competition between structural rejuvenation and structural relaxation [27,28]. In the inset of Fig. 1(a), spatial distribution of nonaffine squared displacement D_{min}^2 [10] under various sample strain is plotted, from which shear banding evolution is noticeable and mature shear band is visible at strain of 0.2. To investigate the glass state of the shear banding region, the shear viscosity is calculated for the atoms residing in the mature shear band at strain of 0.2. This is addressed via the Green-Kubo methodology [29] which is formulated as $\eta = V/(k_B T) \int_0^\infty \langle \sigma_{\alpha\beta}(t) \cdot \sigma_{\alpha\beta}(0)\rangle dt$. Here, V is the volume of the shear band region, k_B is the Boltzann constant, and T denotes the temperature of the deformed glass. $\langle \sigma_{\alpha\beta}(t) \cdot \sigma_{\alpha\beta}(0)\rangle$ represents the shear auto-correlation function in which $\sigma_{\alpha\beta}(t)$ denotes the off-diagonal components of stress tensor at time t, and $\langle \cdots \rangle$ characterizes the ensemble average. The results are accessible in Fig. 1(b). To directly compare with supercooled liquid, the shear viscosity for annealed sample at glass transition temperature T_g (for this model glass, $T_g = 650$ K) is also given in Fig. 1(b). It is interesting to find that the measured viscosity in the shear band nearly falls within the same range that is obtained at T_g. This agrees well with the experimentally observed great drop

in viscosity of the severely deformed metallic glasses [30–32] and evidently demonstrates that the glass state in shear band is equivalent to the supercooled liquid.

More evidence to relate shear band and glass transition is in light of the enthalpy fluctuation. It is widely reported in the literature that the discontinuity in the derivative of the enthalpy-temperature curve, manifesting as the extensively observed overshoot of heat capacity, is a key indicator of the thermal glass transition [33–35]. Following in this strategy, we demonstrate the strain dependence of enthalpy during shear loading, as shown in Figs. 1(c) and 1(d). By analogy, Fig. 1(c) shows the similar discontinuity in the enthalpy-strain curve. More interesting, such discontinuity takes place in the vicinity of shear banding. To be more specific, the derivative of enthalpy with respect to sample strain is directly plotted in Fig. 1(d), in which the red star marks the transition point akin to the capacity step [36] in the thermal glass transition. The similar thermodynamical correspondence offers strong clues for the correlation between shear banding and glass transition.

In addition, the discussion about the consistence between glass transition as well as shear banding can also be traced back to the structural evolution. This is motivated by the previous observation that yielding and glass transition share the same value of critical free volume [37]. It has also been extensively reported in simulated works that glass transition

is accompanying the generation or annihilation of a stiff backbone [38,39], which is usually characterized as instantaneous interpenetration of icosahedral clusters in specific Cu-Zr systems [40,41]. To quantify such structural transition, we monitor the connection of full icosahedrons by defining a dimensionless interpenetrating factor, i.e., S_{max}/S_{all}. Here S_{max} denotes the number of icosahedrons participating in the maximum interpenetrating cluster, while S_{all} is the total number of icosahedrons. In this sense, S_{max}/S_{all} quantifies the degree of interpenetration. The sudden escalation or drop of S_{max}/S_{all} is conceivably able to catch the formation or collapse of icosahedron network, respectively. The disruption of the icosahedral network is reminiscent of the previous simulated works [42,43] which extensively discussed the local structural excitation activated mainly in nonicosahedral regions and its spanning behavior during deformation. Here, the effects of temperature and strain on S_{max}/S_{all} are shown in Figs. 1(e) and 1(f), respectively. Intriguingly, both of them exhibit the typical transition phenomena. It elucidates the similar structural origin between shear banding and glass-to-liquid transition.

Next, the relaxation process, acting as the principal source of information about the dynamics of glass transition [34,44], is investigated for deformed $Cu_{50}Zr_{50}$ glass with varying sample strain. To quantify the relaxation dynamics, deformed samples are further relaxed under conditions with the thermostat turned off to avoid thermal influence induced by artificial effects [45,46]. Then the self-intermediate scattering function is calculated with the generalized form as $F_s(q, t) = 1/N \sum_j^N \langle \exp\{-i\vec{q} \cdot [\vec{r}_j(t) - \vec{r}_j(0)]\}\rangle$. Here $\vec{r}_j$ is the position of jth atom and $\vec{q}$ is the wavevector which is set to be the first peak of the static structure factor. Here, our main scope is the shear banding evolution, thereafter, N denotes the number of atoms in the shear band region. Figures 2(a) and 2(b) show the typical $F_s(q, t)$ responses as a function of time for various applied strains. Generally, it is seen that $F_s(q, t)$ shows a decay behavior from one at the initial time, and then dramatically drops down at a specific timescale. It is apparent from Fig. 2(a) that the increase of sample strain accelerates the decay rate. This implies that severe deformation is equivalent to thermal activation energy on enhancing the atomic mobility as well as inducing the anticipated rejuvenated state [47–49]. Such a positive effect is out of operation in the vicinity of shear banding occurrence. As shown in Fig. 2(b), $F_s(q, t)$ nearly collapses to one single curve after the imposed strain exceeding a certain value of 0.135. It indicates that the deformation process can be separated into two regimes. In the first regime, relaxation response is significantly sensitive to applied strain while it changes to strainindependent in the second regime. Such change of the relaxation behavior suggests the dynamic crossover at strain of 0.135. This dynamic crossover can be further certified by the structure relaxation time τ_α which is defined from $F_s(q, \tau_\alpha) = e^{-1}$ as marked by the orange dashed line in Fig. 2. Here, τ_α for different imposed strains are given in Fig. 2(c). It should be noted that the relaxation time in atomistic simulation is about several orders of magnitude lower than that in experiments. This is attributed to the higher cooling rates and limited physical times of the quench process, causing the less relaxed glass obtained in simulations [50]. It is found that τ_α shows a
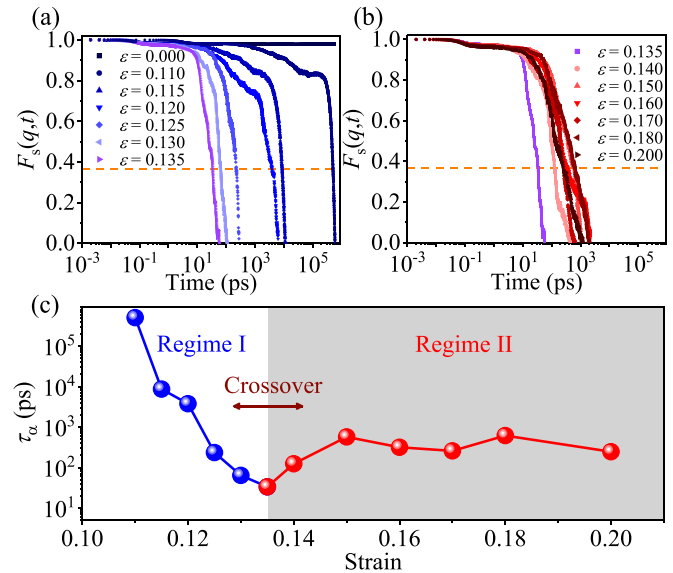

FIG. 2. Dynamical crossover of glass state under external strain. (a), (b) Self-intermediate scattering function for configurations experienced various applied strains. The results are obtained by using atoms in the shear band region. Here, horizontal dashed line colored orange characterizes e^{-1} which is used to define the α-relaxation time τ_α. (c) α-relaxation time as a function of sample strain.

decreasing trend with strain (ε) for $\varepsilon < 0.135$; nevertheless, τ_α nearly maintains constant for $\varepsilon > 0.135$. The inflection point, i.e., $\varepsilon = 0.135$, is thus the critical timescale of dynamic crossover. Referring back to Fig. 1(a), such critical strain is in the vicinity of yielding points. In this regard, it is conceivable that dynamic crossover is the characteristic nature of shear instability as well as subsequent occurrence of shear bands. It is noted that the imposed strain is in plastic regime, leading to the much faster relaxation process of stressed glass than the previous work [51] where a nominally elastic regime is considered. Since the main scope is the onset of shear banding, such relaxation time is accessible via the classical MD simulations. To investigate the thermally activated local structural excitations [42,43] and slow relaxation process at experimental timescales, it is more appropriate to consider long-time scale simulations [52,53] or accelerated simulations like metadynamics [15,54].

Having elaborated above the phenomenological linkage, it is now in pressing need to provide direct comparisons between theoretical predictions, especially from classical thermal glass transition criterion, and simulated data from shear banding. To address this issue, we introduce the recently developed local configurational temperature T_c [46] that is defined as the derivative of the configurational potential energy with respect to the two-body excess entropy, S_2 [55]. First of all, we identify the evolution of configurational temperature for atoms inside the shear band. As shown in Fig. 3(a), T_c monotonously increases with growing applied strains before reaching the dynamical crossover point at strain 0.135. For the sake of simplicity, T_c is reduced by the maximum value at strain of 0.135 in the overall analysis of this paper. Since it has been demonstrated in Fig. 2(c) that the dynamical crossover point is the end of burst of dynamics, we focus our scope on the
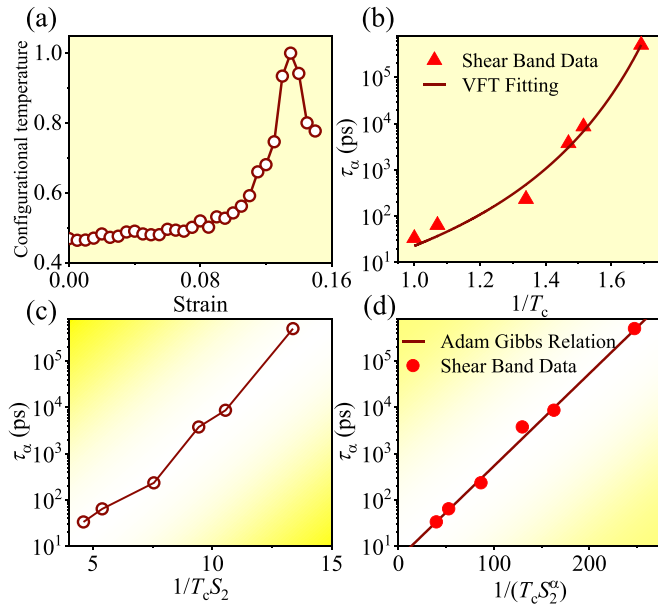
FIG. 3. Validation of VFT law and Adam-Gibbs relation. (a) The configurational temperature, reduced by the maximum value at $\varepsilon = 0.135$, as a function of applied strain. (b) α-relaxation time as a function of inverse configurational temperature. The solid line is the best fit according to VFT equation. (c) Standard Adam-Gibbs plot shows the variation of τ_α with increasing $1/(T_c S_2)$. (d) The modified Adam-Gibbs relation with α as a correction factor to fit the data obtained from shear band region.

FIG. 4. (a) Evolution of per atom potential energy during external loading. (b) The zoom in plot of the profile of the typical hopping to a new "meta-basin" induced by applied strain in (a).

process of structural disordering prior to yielding at $\varepsilon = 0.135$. In this regime, we test the empirical Vogel-Fulcher-Tammann (VFT) equation on the shear banding process via studying the effects of configurational temperature on the glass state characterized by the τ_α.

Figure 3(b) shows that the VFT law provides a good description of the dependence of α-relaxation time on inverse configurational temperature. Furthermore, we test the venerable theory of the glass formation, i.e., the Adam-Gibbs relation [20], which takes advantage of the fact that glass transition is accompanied by variation in configurational entropy which is temperature dependent and controls the growth of the relaxation time [56–58]. Following a simple and intuitive formulation, the standard Adam-Gibbs theory yields $\log(\tau_\alpha/\tau_0) \propto 1/(T S_{\mathrm{conf}})$ where τ_0 is a microscopic time scale and S_{conf} denotes the configurational entropy. Since the limits of exact expression of S_{conf}, we use the two-body term S_2 which is proved to account for about 90% of the configurational entropy [59,60]. We present the results of shear band data by collecting the $1/(T_c S_2)$ relevance of α-relaxation time, as shown in Fig. 3(c). Here, the value of S_2 is reduced with the unstressed glass as the reference state, i.e., $S_2 = 0$ for $\varepsilon = 0$. Figure 3(c) shows that the log plot of α-relaxation time reveals a strong positive correlation with the $1/(T_c S_2)$. However, slight violations from expected straight lines is also seen, which suggests that the standard Adam-Gibbs relation is not completely obeyed over this regime. Such deviation from the Adam-Gibbs plot has already been reported in the context of thermal glass transition [50,61] and has been attributed to the imprecise estimate of the
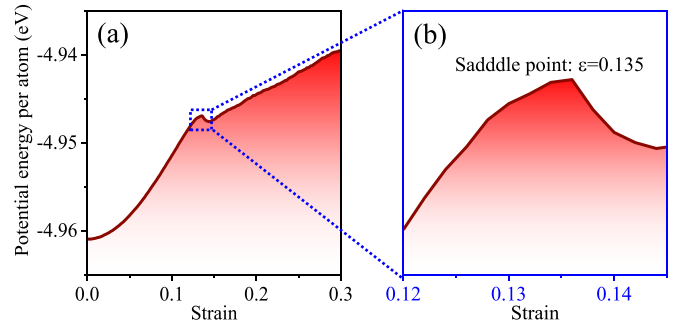
configurational entropy [62] or the generic nature of glassy dynamics [50]. Ref. [50] has reported a more generalized version of the Adam-Gibbs relation as $\log(\tau_\alpha/\tau_0) \propto 1/(T S_{\mathrm{conf}}^\alpha)$, with a nontrivial exponent α acting as an additional free fitting parameter to correct this violation or specifically to correct the entropy contribution to glass-to-liquid transition. This is evident from Fig. 3(d) in which the linear behavior is recovered with the case for the generalized Adam-Gibbs model [50]. Therefore, the emerging picture of the Adam-Gibbs scenario being well-obeyed in the process of shear banding emergence reinforces the robustness of the resemblance between shear banding and glass-to-liquid transition. Also, the critical role of configurational temperature on shear banding is clearly clarified. The increase of configurational temperature can be correlated with excess configurational entropy, and thus provides a driving force for structural disordering. This is equivalent to that of thermal temperature on the glass transition.

Plastic deformation is expected to occur through irreversible hopping between the neighboring basins in the potential energy landscape (PEL) [63–65]. In Fig. 4(a), we depict the evolving potential energy against the applied strain, increasing loading leads to the structural state with enhanced energy. However, this growing trend is transitorily broken as manifestation of the emergent hopping and relaxation process in the vicinity of yielding. Such phenomena are more conspicuous in terms of the close-up view of this part, as shown in Fig. 4(b). It is noted that this result is obtained from a mean-field calculation, which assumes the glass escaping from the initially largescale deep metabasin. It suggests that shear banding behavior corresponds to the transitions among metabasins in PEL. Additionally, one can visualize that the saddle point of this hopping overlaps with the dynamic crossover shown in Fig. 2. This observation gives rise to the natural connection between energy perspective and glass dynamics being the two sides of the same coin—shear banding in amorphous solids.

In conclusion, we have unveiled the intimate linkage between shear banding and glass-to-liquid transition by means of detailed characterizations of viscosity drop, enthalpy fluctuation, structural evolution, as well as dynamical crossovers that are observed at the onset of shear bands. Such predicted correlation is further quantitatively supported via the validation of the VFT equation and the Adam-Gibbs relation

on the configurational temperature effect of the shear banding procedure. The observed effect lays the groundwork for studying the rheology of disordered solids and glass transitions in a unified framework, thus opening a path toward better understanding of the material softening mechanism and physical process of shear band emergence in amorphous solids.

[1] C. A. Schuh, T. C. Hufnagel, and U. Ramamurty, Acta Mater. **55**, 4067 (2007).

[2] M. L. Falk and J. Langer, Annu. Rev. Condens. Matter Phys. **2**, 353 (2011).

[3] A. Greer, Y. Cheng, and E. Ma, Mater. Sci. Eng. R **74**, 71 (2013).

[4] A. Nicolas, E. E. Ferrero, K. Martens, and J.-L. Barrat, Rev. Mod. Phys. **90**, 045006 (2018).

[5] S. A. Rogers, D. Vlassopoulos, and P. T. Callaghan, Phys. Rev. Lett. **100**, 128304 (2008).

[6] A. Furukawa and H. Tanaka, Nat. Mater. **8**, 601 (2009).

[7] F. Spaepen, Acta Metall. **25**, 407 (1977).

[8] A. Lemaître, Phys. Rev. Lett. **89**, 195503 (2002).

[9] A. S. Argon, Acta Metall. **27**, 47 (1979).

[10] M. L. Falk and J. S. Langer, Phys. Rev. E **57**, 7192 (1998).

[11] V. Hieronymus-Schmidt, H. Rösner, G. Wilde, and A. Zaccone, Phys. Rev. B **95**, 134111 (2017).

[12] D. Klaumünzer, A. Lazarev, R. Maaß, F. H. Dalla Torre, A. Vinogradov, and J. F. Löffler, Phys. Rev. Lett. **107**, 185502 (2011).

[13] Z. Lu, W. Jiao, W. H. Wang, and H. Y. Bai, Phys. Rev. Lett. **113**, 045501 (2014).

[14] Z. L. Tian, Y. J. Wang, Y. Chen, and L. H. Dai, Phys. Rev. B **96**, 094103 (2017).

[15] P. Cao, K. A. Dahmen, A. Kushima, W. J. Wright, H. S. Park, M. P. Short, and S. Yip, J. Mech. Phys. Solids **114**, 158 (2018).

[16] G. Zhang, S. A. Ridout, and A. J. Liu, Phys. Rev. X **11**, 041019 (2021).

[17] Z. Y. Yang, Y. J. Wang, and L. H. Dai, Phys. Rev. Res. **4**, 023220 (2022).

[18] Y. H. Liu, C. T. Liu, W. H. Wang, A. Inoue, T. Sakurai, and M. W. Chen, Phys. Rev. Lett. **103**, 065504 (2009).

[19] P. Guan, M. Chen, and T. Egami, Phys. Rev. Lett. **104**, 205701 (2010).

[20] G. Adam and J. H. Gibbs, J. Chem. Phys. **43**, 139 (1965).

[21] S. Plimpton, J. Comput. Phys. **117**, 1 (1995).

[22] M. I. Mendelev, Y. Sun, F. Zhang, C. Z. Wang, and K. M. Ho, J. Chem. Phys. **151**, 214502 (2019).

[23] See Supplemental Material at http://link.aps.org/supplemental/10.1103/PhysRevMaterials.6.L100602 for details of the atomistic simulations.

[24] S. Nosé, J. Chem. Phys. **81**, 511 (1984).

[25] M. Parrinello and A. Rahman, J. Appl. Phys. **52**, 7182 (1981).

[26] Z. Y. Yang, Y. J. Wang, and L. H. Dai, Scr. Mater. **162**, 141 (2019).

[27] J. Lu, G. Ravichandran, and W. L. Johnson, Acta Mater. **51**, 3429 (2003).

[28] L. T. Zhang, Y. J. Wang, Y. Yang, and J. C. Qiao, Sci. China: Phys., Mech. Astron. **65**, 106111 (2022).

[29] M. P. Allen and D. J. Tildesley, *Computer Simulation of Liquids* (Clarendon Press, Oxford, 1987).

[30] J. C. Ye, J. Lu, C. T. Liu, Q. Wang, and Y. Yang, Nat. Mater. **9**, 619 (2010).

[31] R. Maaß, D. Klaumünzer, G. Villard, P. M. Derlet, and J. F. Löffler, Appl. Phys. Lett. **100**, 071904 (2012).

[32] Z. Liu, Y. Yang, and C. Liu, Acta Mater. **61**, 5928 (2013).

[33] C. A. Angell, Science **267**, 1924 (1995).

[34] J. C. Dyre, Rev. Mod. Phys. **78**, 953 (2006).

[35] H. L. Smith, C. W. Li, A. Hoff, G. R. Garrett, D. S. Kim, F. C. Yang, M. S. Lucas, T. Swan-Wood, J. Y. Y. Lin, M. B. Stone, D. L. Abernathy, M. D. Demetriou, and B. Fultz, Nat. Phys. **13**, 900 (2017).

[36] H. B. Ke, P. Wen, and W. H. Wang, AIP Adv. **2**, 041404 (2012).

[37] H. B. Ke, P. Wen, D. Q. Zhao, and W. H. Wang, Appl. Phys. Lett. **96**, 251902 (2010).

[38] H. W. Sheng, W. K. Luo, F. M. Alamgir, J. M. Bai, and E. Ma, Nature (London) **439**, 419 (2006).

[39] M. Li, C. Z. Wang, S. G. Hao, M. J. Kramer, and K. M. Ho, Phys. Rev. B **80**, 184201 (2009).

[40] R. Soklaski, Z. Nussinov, Z. Markow, K. F. Kelton, and L. Yang, Phys. Rev. B **87**, 184203 (2013).

[41] E. Ma and J. Ding, Mater. Today **19**, 568 (2016).

[42] P. M. Derlet and R. Maaß, J. Mater. Res. **32**, 2668 (2017).

[43] P. M. Derlet and R. Maaß, Acta Mater. **143**, 205 (2018).

[44] L. Wang, N. Xu, W. H. Wang, and P. Guan, Phys. Rev. Lett. **120**, 125502 (2018).

[45] N. P. Bailey, J. Schiøtz, and K. W. Jacobsen, Phys. Rev. B **73**, 064108 (2006).

[46] Z. Y. Yang and L. H. Dai, Phys. Rev. Mater. **5**, 123602 (2021).

[47] Y. H. Sun, A. Concustell, and A. L. Greer, Nat. Rev. Mater. **1**, 16039 (2016).

[48] A. Barbot, M. Lerbinger, A. Lemaître, D. Vandembroucq, and S. Patinet, Phys. Rev. E **101**, 033001 (2020).

[49] S. S. Schoenholz, E. D. Cubuk, D. M. Sussman, E. Kaxiras, and A. J. Liu, Nat. Phys. **12**, 469 (2016).

[50] M. Ozawa, C. Scalliet, A. Ninarello, and L. Berthier, J. Chem. Phys. **151**, 084504 (2019).

[51] P. M. Derlet and R. Maaß, Acta Mater. **209**, 116771 (2021).

[52] P. M. Derlet and R. Maaß, J. Alloys Compd. **821**, 153209 (2020).

[53] P. M. Derlet, H. Bocquet, and R. Maaß, Phys. Rev. Mater. **5**, 125601 (2021).

[54] Y. J. Wang, J. P. Du, S. Shinzato, L. H. Dai, and S. Ogata, Acta Mater. **157**, 165 (2018).

[55] P. M. Piaggi and M. Parrinello, J. Chem. Phys. **147**, 114112 (2017).

[56] J. C. Dyre, T. Hechsher, and K. Niss, J. Non-Cryst. Solids **355**, 624 (2009).

[57] S. Sengupta, S. Karmakar, C. Dasgupta, and S. Sastry, Phys. Rev. Lett. **109**, 095705 (2012).

[58] D. Han, D. Wei, J. Yang, H. L. Li, M. Q. Jiang, Y. J. Wang, L. H. Dai, and A. Zaccone, Phys. Rev. B **101**, 014113 (2020).

[59] A. Baranyai and D. J. Evans, Phys. Rev. A **40**, 3817 (1989).

[60] T. S. Ingebrigtsen and H. Tanaka, Proc. Natl. Acad. Sci. **115**, 87 (2018).

[61] K. L. Ngai, J. Phys. Chem. B **103**, 5895 (1999).

[62] C. M. Roland, S. Capaccioli, M. Lucchesi, and R. Casalini, J. Chem. Phys. **120**, 10640 (2004).

[63] W. L. Johnson and K. Samwer, Phys. Rev. Lett. **95**, 195501 (2005).

[64] J. S. Harmon, M. D. Demetriou, W. L. Johnson, and K. Samwer, Phys. Rev. Lett. **99**, 135502 (2007).

[65] Y. Fan, T. Iwashita, and T. Egami, Phys. Rev. Lett. **115**, 045501 (2015).